HHS Public Access

Author manuscript

Biochemistry. Author manuscript; available in PMC 2021 November 26.

Published in final edited form as:

Biochemistry. 2017 May 02; 56(17): 2282–2293. doi:10.1021/acs.biochem.7b00034.

Molecular recognition in mitochondrial cytochromes P450 that catalyze the terminal steps of corticosteroid biosynthesis

Hwei-Ming Peng[†], **Richard J. Auchus**[*,†]

[†]Division of Metabolism, Endocrinology, & Diabetes, Department of Internal Medicine and Department of Pharmacology, Ann Arbor, MI 48109, United States

Abstract

The mitochondrial cytochromes P450 11B1 and P450 11B2 are responsible for the final stages of cortisol and aldosterone synthesis, respectively. Dysregulation of both enzymes have been implicated in secondary forms of hypertension. Molecular recognition of the cytochromes P450 with their corresponding redox partner is a key step in the catalytic cycle, yet the precise nature of the interaction of P450 11B1 or P450 11B2 with their proximal partner adrenodoxin (Adx) is still unknown. Here, we obtained complexes of P450 11B1•Adx_2 and P450 11B2•Adx_2 using the zero-length cross-linker ethyl-3-(3-dimethylamino-propyl) carbodiimide, which formed best under low ionic-strength conditions. R-to-K mutations were introduced in the P450s at residues predicted to form salt bridges with Adx and allow cross-linking with carbodiimide reagent. Mass spectrometric analysis of the chymotrypsin digested-ternary complexes identified seven cross-linked peptide pairs. Consistent with the electrostatic interaction of K370 in P450 11B1-WT and K366 in P450 11B2-R366K with D79 of Adx, Adx mutation L80K abolished complex formation. Using these sites of interaction as constraints, protein-docking calculations based on the crystal structures of the two proteins yielded a structural model of the P450 11B1•Adx_2 complex. The appositional surfaces include R/K366, K370, and K357 of P450 11B1, which interact with D79, D76, and D113 (second molecule) of Adx, respectively. Similar to P450 11B1, P450 11B2 also forms a complex with the Adx dimer via three lysine residues. We describe similarities and differences in our models of the P450 11B1/11B2•Adx_2 complexes with the structure of the P45011A1-Adx fusion protein.

Graphical Abstract

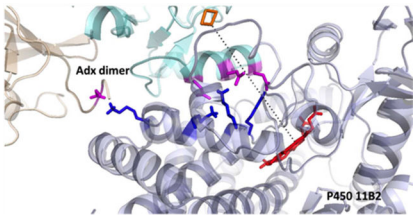

[*]Corresponding author: Tel 734-764-7764, FAX 734-936-6684, rauchus@med.umich.edu.

Keywords

cytochrome P450 11B1; cytochrome P450 11B2; adrenodoxin; protein cross-linking; mass spectrometry; cortisol; aldosterone; mitochondrion

The human adrenal cortex contains two distinct mitochondrial cytochrome P450s with 11β-hydroxylase activity. The cognate genes for these two highly homologous enzymes differ markedly in their regulation in order to fulfill their physiologic functions. The *CYP11B1* gene is expressed in the adrenal zonae fasciculata and reticularis under the control of adrenocorticotropin and encodes the P450 11B1 protein (11β-hydroxylase), which catalyzes the synthesis of cortisol from 11-deoxycortisol. The *CYP11B2* gene is exclusively expressed in the zona glomerulosa under the control of the renin-angiotensin system and intracellular calcium, and the encoded P450 11B2 enzyme (aldosterone synthase) catalyzes all 3 oxygenations required for aldosterone synthesis from 11-deoxycorticosterone (1, 2). Both enzymes contain 503 amino acid residues, but a 24-residue N-terminal mitochondrial targeting sequence is cleaved off after translocation into the mitochondria to yield the mature proteins. The additional 18-hydroxylase and 18-oxidase activities of P450 11B2 derive from 31 amino-acid differences in their mature forms. Previous work has demonstrated that substitution of amino acid S288G in P450 11B1 adds efficient 18-hydroxylase activity, and the additional substitution V320A confers the 18-oxidase activity required for aldosterone synthesis (3, 4).

Mutations in *CYP11B1* cause 11β-hydroxylase deficiency, a rare form of congenital adrenal hyperplasia, which is characterized by androgen excess and hypertension (5). In contrast, aldosterone synthase deficiency, which results from *CYP11B2* mutations, presents in infants with life-threatening hypotension and electrolyte imbalances, including hyperkalemia (6). Disorders of adrenal hyperfunction are more common than rare genetic deficiencies and cause significant morbidity if untreated. Cushing syndrome and primary aldosteronism refer to autonomous overproduction of cortisol and aldosterone, respectively. Cushing syndrome promotes glucose intolerance and bone loss; primary aldosteronism is the most common cause of secondary hypertension; and even mild forms of both conditions confer higher cardiovascular risk (7, 8). Modulation of adrenal steroids synthesis by inhibiting P450 11B1 or P450 11B2 activity is hence an emerging pharmacological approach for these diseases. Osilodrostat was designed to block P450 11B2, lower aldosterone production, and thus treat hypertension, but the drug also potently inhibits P450 11B1, which prompted its repurposing to treat Cushing disease (9, 10) and illustrates the difficulty in developing selective inhibitors for these similar enzymes.

Given their high homology and common substrates for 11β-hydroxylation chemistry, the divergent spectrum of subsequent activities and vastly different physiologic functions of these two P450 11B enzymes presents a paradox that has not been explained. Bovine P450 11B1 is the only 11β-hydroxylase in the cow adrenal yet exhibits aldosterone synthase activity confined to the zona glomerulosa (11). Consequently, additional mechanisms beyond P450 sequence must contribute to the activity profile of these enzymes. For other multi-step P450-reaction pathways, redox partner participation in electron transfer and/or

enzyme structure constitutes a common mechanism for regulating additional activities. For example, P450 17A1 efficiently catalyzes only the 17-hydroxylase reaction in the zona fasciculata, to generate cortisol, but the presence of cytochrome b_5 (b5) in the zona reticularis and gonads activates the 17,20-lyase activity (2, 12). Important residues on P450 17A1 (13, 14) and b5 (15) form specific interactions (16, 17) that increase the coupling of NADPH consumption to androgen formation (18). For P450 11B1 and 11B2, however, detailed structural information about their interactions with redox partners is not available.

The adrenal iron-sulfur protein, adrenodoxin (Adx, also termed ferredoxin-1), is involved in steroid hormone biosynthesis by acting as an electron shuttle between ferredoxin reductase and mitochondrial P450s (19). Mature Adx is a low-molecular-mass (~12 kDa) soluble protein, which is negatively charged at neutral pH and was previously reported to function as a homodimer in electron transfer (20). Although the crystal structures of human P450 11B2 (PDB 4DVQ) (21) and Adx (PDB 3P1M, no PubMed ID) have been elucidated, the structural arrangement of the functional complex between these two proteins remains unknown. The electrostatic association of Adx and P450 11A1 has been investigated (20, 22), and the identification of two salt bridges Lys339 (P450 11A1)-Asp72 (Adx) and Lys343 (P450 11A1)-Asp76 (Adx) from the crystal structure of the fusion protein (PDB: 3N9Y) supports the significance of these interactions (23). In the case of Adx and P450 11B1, however, the hydrophobic properties of the interaction site were reported to be more important than electrostatics (24). Here we probed these protein-protein interactions, using cross-linking coupled with mass spectrometry, mutagenesis, and structural modelling to determine the structures of the P450 11B1•Adx and P45011B2•Adx complexes, to better understand the control of redox-partner interactions for these steroidogenic mitochondrial P450 enzymes.

Experimental Procedures

Materials.

Ampicillin, 5-aminolevulinic acid, isopropyl-β-D-thiogalactopyrano-side (IPTG), Octyl-sepharose CL-4B, and His-Select resin were obtained from Sigma (St Louis, MO). Ethyl-3-(3-dimethylaminopropyl) carbodiimide (EDC) was obtained from Pierce (Rockford, IL). Tween-20 and plasmid pGro7 were purchased from Thermo Fisher Scientific (Waltham, MA). Ni-NTA resin was obtained from Qiagen (Valencia, CA). Cholate was obtained from Chem-Impex International (Wood Dale, IL). PVDF membrane was obtained from Millipore (Billerica, MA); Clarity Western ECL reagent was obtained from Bio-Rad (Richmond, CA); and Blue Devil autoradiography film was acquired from Genesee Scientific (San Diego, CA). The mouse anti-His tag antibody was obtained from GenScript (Piscataway, NJ) and used at 1:1500 dilution, and secondary goat anti-mouse IgG-HRP antibody conjugate (Thermo Fisher Scientific) was used at 1:8000 dilution. Complete mini-protease inhibitor was obtained from Roche Diagnostics (Indianapolis, IN). Bactotryptone and yeast extract were purchased from Difco (Detroit, MI). Molecular biology reagents, including restriction enzymes and ligases, were obtained from New England BioLabs (Beverly, MA). Platinum *Pfx* DNA polymerase was obtained from Life Technologies (Grand Island, NY). The cDNA

of human Adx, CYP11B1, CYP11B2, and ferredoxin reductase were kindly provided by Prof. Walter L. Miller, University of California, San Francisco.

Plasmid Construction.

A cDNA encoding human CYP11B1 or CYP11B2 in pcDNA3 was amplified by PCR to remove 24-amino acid N-terminal mitochondria-targeting sequence and to add a His_6-tag at the C-terminus. The primers were: 11B1-sense 5'-ATACATATGGCGACCAAAGCGGCGCGGGTCCCCAGGACAGTGCT-3'; 11B1-antisense 5'-AGAATTCTCAGTGATGGTGATGGTGATGGTTGATGGCTCTGAA-3'; 11B2-sense 5'-ATACATATGGCGACCAAAGCGGCGCGGGCCCCTAGGACGGTGCT-3'; and 11B2- antisense 5'-AGAATTCTCAGTGATGGTGATGGTGATGGTTAATCGCTCTGAA-3'. The PCR products were then cloned into pET-17b vector via *Nde*I/*Eco*RI restriction sites. The cDNA for ferredoxin reductase was amplified by PCR to include His_6-tag at the C-terminus and cloned into pET-17b via *Nde*I/*Eco*RI restriction sites. The primers were: FdR-sense 5'-ATACATATGGCGTCTACCCAGGAAAAGACCCCACAG-3'; and FdR-antisense 5'-AGAATTCTCAATGGTGATGGTGATGGTGGTGGCCCAGGAGGCGCA-3'. The sequence coding for mature human Adx (amino acids 62–184) was amplified by PCR to include His_6-tag at the N-terminus and cloned into pLW via *Nco*I/*Eco*RI restriction sites. The primers were: Adx-sense 5'-TATACCATGGCACACCATCACCATCACCATTCATCAGAAGATAAAATAACAGTC-3', and Adx-antisense 5'-ATGAATTCTCAGGAGGTCTTGCCCAC-3'. QuikChange site-directed mutagenesis was used to generate the L80K mutation for Adx and the R366K mutations for P450 11B1 and 11B2. Tandem Adx sequences were constructed by overlapping PCR with different numbers of glycine-rich (GGS) repeats linking two copies of the Adx sequence. Seven or 14 repeats of the GGS motif were placed between the two core sequences and cloned into pLW via *Nco*I/*Eco*RI restriction sites. For Adx-GGS_7-Adx, the primers were: GGS_7-sense 5'-GGAGGTTCTGGAGGTGGATCCTCATCAGAAGATAAA-3', and GGS_7-antisense 5'-TTCTGATGAGGATCCACCTCCAGAACCTCCGGAGGTCTTGCCCAC-3'. For Adx-GGS_{14}-Adx, the primers were: GGS_{14}-sense 5'-GGATCCTCATCAGAAGATAAA-3', and GGS_{14}-antisense 5'-TGATGAGGATCCACCTCCAGAACCTCCGGATCCACCTCCAGAACCTCCGGAGGTCTT-3'. The sequence of the entire coding region and presence of the desired mutation in each plasmid was confirmed by DNA sequencing.

Protein Expression in *Escherichia coli* and Purification.

Human Adx and fused Adx dimers were expressed in *E. coli* strain C41(DE3) and purified as described before (25). Human ferredoxin reductase (26), P450 11B1(27), and P450 11B2 (28) were expressed in C41(DE3) with pGro7 and purified as described previously. Briefly, Fernbach flasks containing 1 liter of Terrific Broth (supplemented with 0.5 mM 5-aminolevulinic acid for P450 11B1/11B2) with 100 μg/mL ampicillin were inoculated with 20 mL of an overnight pre-culture. The cells were grown at 37 °C with shaking at 250 rpm until the A_{600} reached 1.0–1.4 AU, at which time the culture was induced with 0.4 mM IPTG (supplemented with 4g/L arabinose for ferredoxin reductase and P450s) and grown for

20–48 h at 28°C. After cell lysis with French press in buffer A (sterile phosphate-buffered saline (PBS) containing 20% glycerol for ferredoxin reductase and P450s), the recombinant P450 proteins were solubilized using 1% cholate and 1% Tween 20. After centrifugation at 70,000 × *g* for 18 min, the supernatant was mixed with 3–5 mL Ni-NTA affinity resin, and polyhistidine-tagged proteins were eluted with 10 mL 250 mM imidazole, followed by buffer exchange using PD-10 columns. The proteins were further purified with Octyl-sepharose column (2 mL) and subsequently affinity purified with His-Select resin (0.5 mL) according to the manufacturer's protocol. Purified P450 11B1/11B2 preparations showed a specific content of 8–12 nmol P450/mg protein with 3–10% P420.

Reconstituted enzyme assays.

In a 2 mL polypropylene tube, purified human P450 11B1/11B2 (10 pmol, WT or R366K) was mixed with equal amount of ferredoxin reductase, 40-fold molar excess of Adx (WT or L80K), and dilauroylphosphatidyl choline in <10 μL volume and incubated for 5 min. The reaction mixture was then diluted to 0.2 mL with 50 mM HEPES buffer (pH = 7.4), 10 mM $MgCl_2$, 0.2% Tween 20, and substrates 11-deoxycorticosterone (200 μM, for 11β-hydroxylase activity). The resulting mixture was pre-incubated at 37 °C for 3 min before adding NADPH (1 mM) and incubating at 37 °C for another 20 min. The reaction mixture was extracted with 1 mL dichloromethane, and the organic phase was dried under nitrogen flow.

Chromatography, data acquisition, and determination of kinetic constants.

Reaction products were analyzed using an Agilent 1260 Infinity HPLC system with UV detector. Extracted steroid products were dissolved in 20 μL of methanol, and 5 μL injections were resolved with a 50 × 2.1 mm, 2.6 μm, biphenyl 100 Å column (Phenomenex, Torrance, CA), equipped with a guard column at a flow rate of 0.4 mL/min. A methanol/water linear gradient was used: 32.5% to 88.3% methanol from 0 to 10.6 min, 88.3% to 12 min, 99.1% from 12.1 min to 14 min, and 32.5% from 14.1 min to 15 min. Products were identified by retention times of external standards chromatographed at the beginning and ends of the experiments, and the data were processed with Laura4 software (LabLogic) and graphed with GraphPad Prism 6 (GraphPad Software, San Diego, CA).

Cross-linking and Immunoblot Experiments.

Purified human CYP11B1 (25 pmol, WT or R366K), Adx (WT or L80K) were reconstituted at a molar ratio of 1:20. After incubation for 5 min at 25°C, freshly prepared EDC was added to a final concentration of 2 mM in a total volume of 20 μL containing 5–50 mM potassium phosphate (pH 7.0). The mixture was shaken gently at room temperature for 2 h, followed by adding an equal volume of Laemmli sample buffer and boiling for 5 min. Control incubations without EDC were conducted in parallel. The cross-linked proteins were resolved with SDS-PAGE on 4–20% gradient gels, and the bands corresponding to the heterocomplex were excised and submitted to LC-MS/MS analysis at MSBioworks (Ann Arbor, Michigan). For immunoblot analyses, the SDS-PAGE gels were electroblotted onto PVDF membrane. The membranes were blocked for 1 h at room temperature in PBS containing 5% fat-free milk plus 0.1% Tween-20 and were incubated overnight at 4°C with mouse anti-His tag antibody, followed by incubation with secondary antibody for 1 h at

room temperature. The blots were incubated for 1 min with ECL reagent and exposed to photographic film.

LC-MS/MS analysis.

The excised gels containing cross-linked proteins were processed by in-gel digestion using a robot (ProGest, DigiLab) and sequencing-grade chymotrypsin at 37°C for 18 h. The digested sample was analyzed by nano LC-MS/MS with a Waters NanoAcquity HPLC system interfaced to a ThermoFisher Q Exactive tandem mass spectrometer. Peptides were loaded on a trapping column and resolved on a 75 μm analytical column at 350 nL/min; both columns were packed with Jupiter Proteo resin (Phenomenex). The mass spectrometer was operated in data-dependent mode, with MS and tandem MS performed in the Orbitrap at 70,000 FWHM and 17,500 FWHM resolutions, respectively. The fifteen most abundant ions were selected for tandem MS.

Data Processing.

Data were searched using a local copy of Mascot, and the DAT files were parsed into scaffold software for validation, filtering, and creating a non-redundant list for each sample. MS data are loaded as standard Mascot generic file (mgf), and the cross-linked products were identified by Mass Matrix version 2.4.2 (29). The quality of peptide match was evaluated by three validated statistical measures as follows: pp, probabilistic score based on number of matched peaks; pp_2, probabilistic score based on ion intensity distribution of matched peaks; pp_{tag}, probabilistic score based on consecutiveness of matched peaks. A peptide match with maximum (pp and pp_2) >3.7 and pp_{tag} >1.3 was considered to be significant with a p value of <0.05. The settings of Mass Matrix were as follows: (i) enzyme: chymotrypsin; (ii) missed cleavage: 5; (iii) modifications: fixed iodoacetamide derivative of cysteine and variable modifications: deamidation of NQ (DANQ), pyro-Glu from Q (PyrQ), oxidation of M (OxiM), acetylation of N-term (AceB); (iv) precursor ion mass tolerances: 10 ppm; (v) product ion mass tolerances: 0.8 Da; (vi) maximum number of modifications allowed for each peptide: 3; (vii) peptide length: 8–40 amino acid residues; (viii) mass type, monoisotopic; (ix) crosslink, EDC; (x) cross-link mode, exploratory; (xi) maximum number of cross-links per peptide, 2. Mass Matrix adopts a staged search strategy. In the first stage, the tandem mass spectrometric data set was searched against the UniProt database using the target-decoy search strategy for protein identification. Reversed sequences were used as a decoy, and the data were filtrated with a 1% false discovery rate. In the second stage, protein matches selected from the first stage were searched with the search algorithm that Mass Matrix employs to identify the cross-linked peptides (30).

Three-dimensional Model Analysis.

The three-dimensional model of the P45011B1 was built using crystal structures of P450 11B2 (PDB 4DVQ) as a template. Structural modeling was performed using the I-TASSER server based on *ab initio*/threading method (31). The server predicted 5 models of P450 11B1 and the best model was selected based on C-score. C-score is a confidence score for estimating the quality of predicted models by I-TASSER, based on the significance of threading template alignments and the convergence parameters of the structure assembly simulations. Human Adx homodimer PDB file was created by HADDOCK software

tool (32), which is a suite of rigid-body protein-protein docking programs, using the distance constraints of two symmetric intermolecular salt bridges between subunits, R106(A)-D109(B) and D109(A)-R106(B), as in the bovine Adx homodimer structure (PDB 1CJE). The three-dimensional models of P45011B1•Adx_2 and P450 11B2•Adx_2 were then predicted using HADDOCK, which incorporated constraints from cross-linking data. The programs returned the 10 most probable models (clusters) out of thousands of candidates based on their geometry, hydrophobicity, and electrostatic complementarity. The first-ranked model in cluster 1 of HADDOCK was selected as the final model for further analysis. Chains A and B of human Adx dimer molecule described above were set as a single ligand molecule, and chain A of human P450 11B1 or P450 11B2 as receptor molecule. As constraints, the 3 intermolecular cross-links identified below as well as amino acids identified from mutagenesis studies—R/K366, K370, K357 of CYP11B1 and D79, D76, and D113 of Adx—were used during all calculations to predict the interaction of these two target proteins. Molecular graphic figures were generated using PyMOL (http://www.pymol.org/). Molecular interface analysis was performed using PDBePISA (http://www.ebi.ac.uk/pdbe/prot_int/pistart.html).

Results

R-to-K mutations of key P450 11B1 and P450 11B2 residues.

Mutation R366C in CYP11B1 has been identified in patients with partial 11β-hydroxylase impairment (5). This point mutation results in a loss of 77–80% of wild-type activity by eliminating a positive charge in the K-helix and potentially affecting Adx binding. Moreover, a lysine residue (K339), which is present at the corresponding position of human P450 11A1 enzymes, was reported to directly interact with D72 of Adx (23). Therefore, conservative R-to-K mutations in residue 366 of P450 11B1 and 11B2 were strategically constructed in an effort to maintain their activity, yet render the P450 susceptible to chemical reaction with EDC cross-linking agents. The effect of R366K mutation on the 11β-hydroxylase activity of P450 11B1 and 11B2 was investigated by HPLC analysis of the substrate conversion of 11-deoxycorticosterone into corticosterone. The resulting R366K mutations exhibited similar 11β-hydroxylase as wild-type proteins (Fig. 1A). These mutations were then employed with wild-type P450s in cross-linking experiments with Adx.

Point mutation of L80K in Adx.

The acidic region of Adx between residues 72 and 79 in helix α3 has been shown to be the main contact residues for binding to ferredoxin reductase and cytochrome P450 11A1 from site-directed mutagenesis studies (22, 33, 34). L80, mutated in this study, is adjacent to the key residue D79 and highly conserved among vertebrates; in contrast, lysine occupies the analogous position of *E. coli* Adx (35). Substitution of lysine for L80 in human Adx L80K resulted in a remarkable loss (>95%) of its ability to support 11β-hydroxylase activity of P450 11B1 and 11B2 (Fig. 1B), even though L80K displayed identical UV-Vis spectrum as WT and had no effect on electron transfer with ferredoxin reductase (data not shown). These data indicate that hydrophobic residues near D79 in Adx are an important feature of this interaction site and that polar substitutions are poorly tolerated, presumably related to

a steric distortion of the interface. Hence, Adx mutation L80K was included as a negative control in cross-linking experiments.

Chemical Cross-Linking and Optimization of Reaction Conditions.

To trap the transient ternary complex of each P450 with the Adx dimer, EDC was used, a zero-length cross-linker that can form amide bonds between carboxylate groups from aspartate (D) and glutamate (E) side chains to primary amine groups from lysine (K). Treatment of Adx and P450 11B preparations with EDC resulted in two cross-linked species (Fig. 2A, 2B). In the absence of EDC, Adx and P450 11B1/11B2 migrated with apparent molecular masses of 12 kDa and 50 kDa, respectively. Treatment with EDC, however, resulted in the formation of 74-kDa and 24-kDa cross-linked products that were recognized by anti-His antibodies (Fig. 2B). Moreover, the relative amounts of the 74-kDa species increased with increasing Adx (data not shown), and the highest yields were obtained at protein ratios of 1:20 (P450:Adx) in the presence of 5–20 mM potassium phosphate buffer. Further increase in ionic strength leads to complex dissociation (Fig. 2C). The treatment of WT or R366K P450s with EDC generated similar 74-kDa cross-linked products, which is consistent with a 1:2 complex comprising one mitochondrial cytochrome P450 and two Adx molecules. Mutation L80K of Adx was not able to form any complex with P450 11B1/11B2 WT or R366K, consistent with the activity data (Fig. 1B), and the formation of 24-kDa homodimer species was also diminished compared to WT Adx (Fig. 2B).

Mass-spectrometry analysis of protein cross-links.

Following SDS-PAGE and Denville blue staining of the cross-linked species (Fig. 2A), peptide mixtures generated from in-gel chymotrypsin digestions were separated by nano-HPLC and analyzed by tandem mass spectrometry. These digests contained peptides from both P450 11B1/11B2 and Adx, as well as inter- and intramolecular cross-linked products. To identify cross-linked peptides involving the 2 proteins from this intricate mixture, the experimentally obtained monoisotopic masses were compared with calculated masses of peptides and cross-linked products derived from MassMatrix software package (29) as described in the Experimental Procedures. Possible cross-linking sites between the amino acids D to K, and E to K were examined. Seven cross-linked peptides between P450 11B1/11B2 WT or R366K and Adx sequences were identified in multiple experiments (Table 1).

Fig. 3A–C shows the fragmentation spectra for P450 11B1-Adx cross-links: P450 11B1-WT: $_{354}$HPQ<u>K</u>AT$_{359}$ – Adx: $_{110B}$TVA<u>D</u>ARQ$_{116B}$, P450 11B1-WT: $_{366}$RAAL<u>K</u>ET$_{372}$ – Adx: $_{73A}$EENDML<u>D</u>L$_{80A}$, and P450 11B1-R366K: $_{351}$ISEHPQ<u>K</u>A$_{358}$ – Adx: $_{113B}$<u>D</u>ARQ$_{116B.}$ Fig. 4A–D shows the fragmentation spectra for P450 11B2-Adx cross-links: P450 11B2-WT: $_{349}$ASISEHPQ<u>K</u>ATTEL$_{362}$ – Adx: $_{101B}$DNMTVRVPETVA<u>D</u>A$_{114B}$, P450 11B2-R366K: $_{366}$<u>K</u>AALK$_{370}$ – Adx: $_{76A}$DML<u>D</u>LA$_{81A}$, P450 11B2-R366K: $_{366}$KAAL<u>K</u>ETL$_{373}$ – Adx: $_{73A}$EEN<u>D</u>ML$_{78A,}$ and P450 11B2-R366K: $_{360}$TELPLL<u>K</u>A$_{367}$ – Adx: $_{77A}$ML<u>D</u>L$_{80A}$. Given that EDC is a carboxylate-to-amine zero-length cross-linker, these cross-links imply that these paired residues interact by complementary charges and approach within van der Waals contact of each other.

Models of Adx dimer interactions with P450 11B1 and P450 11B2.

Using distance constraints derived from the cross-linking data, low-resolution structural models were calculated using HADDOCK (32, 36, 37) rigid body energy minimization (Fig. 5A–D). The X-ray crystal structure of human P450 11B2 with bound 11-deoxycorticosterone (21) or a P450 11B1 model constructed from the P450 11B2 structure with I-TASSER were used as the receptor molecules (see Experimental Procedures). While crystallographic structures are available for both human and bovine Adx, their dimeric interfaces are not the same, probably due to differences in crystal packing. Only the bovine Adx homodimer structure (20) afforded ternary clusters with both P45011B molecules from HADDOCK simulations; therefore, the human Adx homodimer was first generated with HADDOCK as described in the Experimental Procedures before docking with each P450. The structures of the P450 11B1•Adx_2 and P450 11B2•Adx_2 complexes thus generated from HADDOCK show electrostatic interactions at the interface of the complex between 3 key pairs of amino acids, including K370, R366, and K357 in P450 11B1/11B2 with Adx residues D76 and D79 (A molecule) and D113 (B molecule), respectively, demonstrating that both Adx dimer subunits are required for optimal complex formation with both P450s (Fig. 5A, D). This model incorporates the available evidence and features direct electrostatic and functional interactions between these charged residues. In addition to the three cross-links identified, cationic R453 on P45011B1/11B2 was found to interact with D72 of Adx (A molecule, Fig. 5D, Table 2, and Table 3), which is consistent with a previous study that P450 11B1 mutation R453Q resulted in almost completely absent enzyme activity (38).

Surface contacts analysis by PISA.

To explore further the regions of the protein surfaces that interact, we used the protein interfaces, surfaces and assemblies service PDBePISA at the European Bioinformatics Institute (http://www.ebi.ac.uk/pdbe/prot_int/pistart.html/) to compare the Accessible Surface Area (ASA) of each residue alone and in the ternary complex. PISA analysis of the interactions reveals: (i) the P450 11B1•Adx_2 interaction covers 1344.4 $Å^2$ (5.6% of the P450 11B1 ASA), and (ii) the P450 11B2•Adx_2 interaction covers 1237.2 $Å^2$ (5.5% of the P450 11B2 ASA). The interaction surface shows good shape complementarity with numerous electrostatic interactions, including 18 potential hydrogen bonds and 17 potential salt bridges for P450 11B1 (Table 2, Fig. 5D); and 10 potential hydrogen bonds and 13 potential salt bridges for P450 11B2 (Table 3, Fig. 5D), plus hydrophobic interactions. Interfacing residues identified within the ternary complex including K366/K370 (K-helix), K357 (J'-helix), and R453 (L-helix) in P450 11B1 and P450 11B2 with D72/E73/D76/D79 (α3-helix, A molecule), and D113 (3/10-helix, B molecule) in Adx were all consistent with the results from cross-linking and mutagenesis experiments.

Discussion

We have developed proposed structures of P450 11B1•Adx_2 & P450 11B2•Adx_2 ternary complexes based on results from mutagenesis, activity studies, and chemical cross-linking coupled with mass spectrometry analysis. The closest contacts between P450 11B1 & 11B2 and Adx involve R366, K370, R453 and K357 of P450 with D79, D76, and D72 (A molecule) and D113 (B molecule) of the Adx homodimer. A hydrophobic residue adjacent

to the acidic D79 of Adx is also a mandatory feature, as substitution L80K severely disrupts the redox-partner interaction. Further support for this model derives from patients with 11β-hydroxylase deficiency, where substitution of R366 to C (5), R453 to Q (38), and R454 to C (39) in P450 11B1 prevents binding of Adx and severely impairs 11β-hydroxylase activity. We employed a similar strategy with R-to-K mutations that enabled EDC cross-linking to elucidate the recognition and interactions between P450 17A1 and cytochrome b_5 (16). Interestingly, residue K370 in mitochondrial P450 11B1/11B2, which interacts with D76/D79 of Adx, aligns with residue R358 in microsomal P450 17A1, which interacts with E48/E49 of cytochrome b_5. These residues are located on the K-helix within a basic patch on the proximal surface of class I and class II P450s, respectively, which enable the docking of an acidic partner protein.

Functional Adx homodimer has been proposed to be involved in the electron transfer process from the full-length bovine Adx structure (20); however, whether Adx acts as a monomer or dimer for all mitochondrial P450s is still under debate. At least four electron-transfer mechanisms have been proposed: (A) Shuttle model, monomeric Adx serves as a mobile carrier between ferredoxin reductase and P450 (40, 41); (B) Modified shuttle model, Adx dimer is responsible for the reduction of P450 (20, 42); (C) Cluster model, a ternary 1:1:1 complex ferredoxin reductase•Adx•P450 is formed (43); or (D) a quaternary complex with a 1:2:1 ferredoxin reductase•Adx_2•P450 stoichiometry (43, 44). Of these, the shuttle models are more favorable, since the formation of the ternary or even quaternary complex is unlikely from a structural perspective due to overlapping interaction regions on Adx (Table 5). Our data provide evidence for the molecular recognition of Adx homodimer with the mitochondrial P450s 11B1 and 1B2, which is consistent with the modified shuttle model; however we cannot exclude the possibility that different or multiple mechanisms exist for different redox targets, as Adx deliveries electrons to several mitochondrial P450s.

Multiple sequence alignments of mitochondrial P450s in the region where Adx binds (Table 4) shows that these charged residues are highly conserved among the enzymes from different species. Earlier structural work with P450 11A1 and Adx has identified conserved residues from helices K (K339, K343) to mediate Adx binding (23); however, these residues do not interact with the same residues of Adx as proposed in our models (Table 5). Residues D72 and D76, but not D79 in Adx form salt bridges with K339 and K343 of P450 11A1, which correspond to K366 and K370 in P450 11B1/11B2. Moreover, P450 11A1 was reported to form a complex with Adx monomer, not dimer, possibly due to the constrained nature of the fusion protein. In the current study, substitution of a hydrophobic leucine with a charged lysine in Adx mutation L80K not only disrupts the interaction with P450s but also results in less dimerization *in vitro*, indicating a possible coupling between Adx dimerization and redox partner recognition.

Comparison of the P450 11B2-R366K•Adx_2 model superimposed on the P450 11A1-Adx fusion protein structure (3N9Y) (Figure 6) reveals several significant differences in ion pairings formed between basic residues on the P450 and complementary acidic side chains on Adx (Table 5). In particular, K339 on P450 11A1 at the periphery of the proximal heme face forms a salt bridge with D72 on Adx, while the corresponding K366 on P450 11B2 is closer to D79 and too far away to interact with D72 on the Adx_2 dimer. Instead, the

side chain of R453 on P450 11B2 is well positioned to interact with D72. Most notable is the antiparallel orientations of the α3-helices (amino acids 72 to 79) of Adx or Adx_2 dimer at the interfaces in these two complexes, which changes the distance between the heme and the iron-sulfur clusters. The distances between metal centers are 24.4 and 17.7 Å in P450 11B2-R366K•Adx_2 model and the P450 11A1-Adx fusion protein structure, respectively, consistent with a 5-fold higher electron transfer rate for the reduction of P450 11A1 as compared to P450 11B1 (24). Despite these differences, similar 74-kDa cross-linked products of the P450 11A1•Adx_2 complex were also detected under our experimental conditions (data not shown), indicating that the formation of a ternary complex with Adx_2 dimer might be a general property of oxidized, substrate-free mitochondria P450s.

Nevertheless, C-terminus truncated bovine Adx (4–108) was reported to have increased electron transfer ability (45) and an extremely weak tendency to self-associate (46), suggesting that the additional recognition site at D113 on the B molecule of Adx may be dispensable for its function. Since the self-association of oxidized Adx in solution was confirmed by analytical ultracentrifugation studies, whereas reduced Adx was found to be exclusively monomeric (46), the D113 binding site might be redox-sensitive and only operative in the oxidized state, as in our study. To this end, we have also constructed 2 single-polypeptide Adx dimers with 7 or 14 amino acid linkers and expressed them in *E. coli*. The recombinant fused Adx dimers were partially functional and showed 13–23% activities compared to WT Adx for 11β-hydroxylation of 11-deoxycorticosterone with P450 11B1 and P450 11B2 (data not shown). Consequently, both Adx monomers and dimers are competent to act as electron carriers and to support catalysis in our reconstituted system, but monomers appear to be more efficient for both P450 11B enzymes. These observations suggest that Adx dimers might bind and dissociate to monomers upon reduction by ferredoxin reductase prior to electron transfer to the P450 in an advanced modified-shuttle mechanism as proposed by Beilke et al. (42, 46).

Other than these steroidogenic P450s, mitochondrial enzymes such as P450 24A1 and P450 27B1 also receive electrons from Adx. P450 24A1 catalyzes sequential hydroxylation and oxidation steps in the catabolism of the 1α,25-dihydroxyvitamin D3, which in turn is produced via the 1α-hydroxylase P450 27B1 from 25-hydroxyvitamin D3 in the kidney. Site-directed mutagenesis and molecular modeling experiments have indicated that acidic residues between positions 72 to 79 of Adx are involved in electrostatic interaction with positively charged residues located on the proximal surface of mouse P450 27B1 (47). In contrast to our model described here, the authors proposed that D76 and D79 of Adx interact with R457 and R458 in the L-helix, respectively, while D72 and E74 are in close contact with K370 and K374 in the K-helix of the complex (Table 5), respectively.

Chemical cross-linking coupled to mass spectrometry provides a useful tool to derive structural information of protein complexes, yet this bottom-up strategy bears some limitations, such as variable spatial resolution due to the inherent imprecision of the few inter-protein distance restraints, and false-positive peptide matches generated from data analysis. Although the data with our P450 and Adx mutations corroborate our conclusions, additional data from complementary biophysical methods will strengthen the validity of the model. In summary, our data demonstrate that the closely related human 11β-hydroxylases,

P450 11B1 and P450 11B2, behave in a similar way in recognition of their redox partner Adx to engage in steroidogenesis. This study presents an internally consistent model for the binding site of P450 11B1/11B2 with dimeric Adx, an important step in elucidating the structural features responsible for the mitochondrial P450-redox partner binding in general. A detailed understanding of these processes might facilitate the modulation of steroid hormone, sterol, and vitamin D biosynthesis.

Acknowledgements

This work was supported by grant R01-GM086596 from the National Institutes of Health (to RJA)

Abbreviations.

Adx	adrenodoxin
EDC	ethyl-3-(3-dimethylaminopropyl) carbodiimide
IPTG	isopropyl-1-thio-β-D-galactopyranoside
MS	mass spectrometry
Ni-NTA	nickel-nitrilotriacetic acid
P450 11B1	cytochrome P450 11B1
P450 11B2	cytochrome P450 11B2
WT	wild-type

References

1. Rainey WE (1999) Adrenal zonation: clues from 11β-hydroxylase and aldosterone synthase, Mol Cell Endocrinol 151, 151–160. [PubMed: 10411330]
2. Miller WL, and Auchus RJ (2011) The molecular biology, biochemistry, and physiology of human steroidogenesis and its disorders, Endocr Rev 32, 81–151. [PubMed: 21051590]
3. Curnow KM, Mulatero P, Emeric-Blanchouin N, Aupetit-Faisant B, Corvol P, and Pascoe L (1997) The amino acid substitutions Ser288Gly and Val320Ala convert the cortisol producing enzyme, CYP11B1, into an aldosterone producing enzyme, Nat Struct Biol 4, 32–35. [PubMed: 8989319]
4. Bottner B, Denner K, and Bernhardt R (1998) Conferring aldosterone synthesis to human CYP11B1 by replacing key amino acid residues with CYP11B2-specific ones, Eur J Biochem 252, 458–466. [PubMed: 9546661]
5. Parajes S, Loidi L, Reisch N, Dhir V, Rose IT, Hampel R, Quinkler M, Conway GS, Castro-Feijoo L, Araujo-Vilar D, Pombo M, Dominguez F, Williams EL, Cole TR, Kirk JM, Kaminsky E, Rumsby G, Arlt W, and Krone N (2010) Functional consequences of seven novel mutations in the CYP11B1 gene: four mutations associated with nonclassic and three mutations causing classic 11β-hydroxylase deficiency, J Clin Endocrinol Metab 95, 779–788. [PubMed: 20089618]
6. Pascoe L, Curnow KM, Slutsker L, Rosler A, and White PC (1992) Mutations in the human CYP11B2 (aldosterone synthase) gene causing corticosterone methyloxidase II deficiency, Proc Natl Acad Sci U S A 89, 4996–5000. [PubMed: 1594605]
7. Iacobellis G, Petramala L, Barbaro G, Kargi AY, Serra V, Zinnamosca L, Colangelo L, Marinelli C, Ciardi A, De Toma G, and Letizia C (2013) Epicardial fat thickness and left ventricular mass in subjects with adrenal incidentaloma, Endocrine 44, 532–536. [PubMed: 23430367]

8. Rossi GP (2011) A comprehensive review of the clinical aspects of primary aldosteronism, Nat Rev Endocrinol 7, 485–495. [PubMed: 21610687]
9. Bertagna X, Pivonello R, Fleseriu M, Zhang Y, Robinson P, Taylor A, Watson CE, Maldonado M, Hamrahian AH, Boscaro M, and Biller BMK (2014) LCI699, a potent 11β-hydroxylase inhibitor, normalizes urinary cortisol in patients with Cushing's disease: results from a multicenter, proof-of-concept study, J Clin Endocrinol Metab 99, 1375–1383. [PubMed: 24423285]
10. Fleseriu M, Pivonello R, Young J, Hamrahian AH, Molitch ME, Shimizu C, Tanaka T, Shimatsu A, White T, Hilliard A, Tian C, Sauter N, Biller BMK, and Bertagna X (2016) Osilodrostat, a potent oral 11β-hydroxylase inhibitor: 22-week, prospective, Phase II study in Cushing's disease, Pituitary 19, 138–148. [PubMed: 26542280]
11. Wada A, Ohnishi T, Nonaka Y, Okamoto M, and Yamano T (1985) Synthesis of aldosterone by a reconstituted system of cytochrome P-45011β from bovine adrenocortical mitochondria, J Biochem 98, 245–256. [PubMed: 4044554]
12. Auchus RJ, Lee TC, and Miller WL (1998) Cytochrome b_5 augments the 17,20-lyase activity of human P450c17 without direct electron transfer, J Biol Chem 273, 3158–3165. [PubMed: 9452426]
13. Geller DH, Auchus RJ, and Miller WL (1999) P450c17 mutations R347H and R358Q selectively disrupt 17,20-lyase activity by disrupting interactions with P450 oxidoreductase and cytochrome b_5, Mol Endocrinol 13, 167–175. [PubMed: 9892022]
14. Lee-Robichaud P, Akhtar ME, Wright JN, Sheikh QI, and Akhtar M (2004) The cationic charges on Arg347, Arg358 and Arg449 of human cytochrome P450c17 (CYP17) are essential for the enzyme's cytochrome b_5-dependent acyl-carbon cleavage activities, J Steroid Biochem Mol Biol 92, 119–130. [PubMed: 15555906]
15. Naffin-Olivos JL, and Auchus RJ (2006) Human cytochrome b_5 requires residues E48 and E49 to stimulate the 17,20-lyase activity of cytochrome P450c17, Biochemistry 45, 755–762. [PubMed: 16411751]
16. Peng HM, Liu J, Forsberg SE, Tran HT, Anderson SM, and Auchus RJ (2014) Catalytically relevant electrostatic interactions of cytochrome P450c17 (CYP17A1) and cytochrome b_5, J Biol Chem 289, 33838–33849. [PubMed: 25315771]
17. Estrada DF, Laurence JS, and Scott EE (2013) Substrate-modulated Cytochrome P450 17A1 and Cytochrome b_5 Interactions Revealed by NMR, J Biol Chem 288, 17008–17018. [PubMed: 23620596]
18. Peng H-M, Im S-C, Pearl NM, Turcu AF, Rege J, Waskell L, and Auchus RJ (2016) Cytochrome b_5 Activates the 17,20-Lyase Activity of Human Cytochrome P450 17A1 by Increasing the Coupling of NADPH Consumption to Androgen Production, Biochemistry 55, 4356–4365. [PubMed: 27426448]
19. Grinberg AV, Hannemann F, Schiffler B, Muller J, Heinemann U, and Bernhardt R (2000) Adrenodoxin: structure, stability, and electron transfer properties, Proteins 40, 590–612. [PubMed: 10899784]
20. Pikuleva IA, Tesh K, Waterman MR, and Kim Y (2000) The tertiary structure of full-length bovine adrenodoxin suggests functional dimers, Arch Biochem Biophys 373, 44–55. [PubMed: 10620322]
21. Strushkevich N, Gilep AA, Shen L, Arrowsmith CH, Edwards AM, Usanov SA, and Park H-W (2013) Structural insights into aldosterone synthase substrate specificity and targeted inhibition, Mol Endocrinol (Baltimore, Md) 27, 315–324.
22. Wada A, and Waterman MR (1992) Identification by site-directed mutagenesis of two lysine residues in cholesterol side chain cleavage cytochrome P450 that are essential for adrenodoxin binding, J Biol Chem 267, 22877–22882. [PubMed: 1429635]
23. Strushkevich N, MacKenzie F, Cherkesova T, Grabovec I, Usanov S, and Park HW (2011) Structural basis for pregnenolone biosynthesis by the mitochondrial monooxygenase system, Proc Natl Acad Sci U S A 108, 10139–10143. [PubMed: 21636783]
24. Beckert V, and Bernhardt R (1997) Specific aspects of electron transfer from adrenodoxin to cytochromes p450scc and p45011β, J Biol Chem 272, 4883–4888. [PubMed: 9030546]

25. Woods ST, Sadleir J, Downs T, Triantopoulos T, Headlam MJ, and Tuckey RC (1998) Expression of catalytically active human cytochrome P450scc in *Escherichia coli* and mutagenesis of isoleucine-462, Arch Biochem Biophys 353, 109–115. [PubMed: 9578606]
26. Tuckey RC, Li W, Shehabi HZ, Janjetovic Z, Nguyen MN, Kim TK, Chen J, Howell DE, Benson HA, Sweatman T, Baldisseri DM, and Slominski A (2011) Production of 22-hydroxy metabolites of vitamin d3 by cytochrome P450scc (CYP11A1) and analysis of their biological activities on skin cells, Drug Metab Disp 39, 1577–1588.
27. Zollner A, Kagawa N, Waterman MR, Nonaka Y, Takio K, Shiro Y, Hannemann F, and Bernhardt R (2008) Purification and functional characterization of human 11β hydroxylase expressed in *Escherichia coli*, FEBS J 275, 799–810. [PubMed: 18215163]
28. Hobler A, Kagawa N, Hutter MC, Hartmann MF, Wudy SA, Hannemann F, and Bernhardt R (2012) Human aldosterone synthase: recombinant expression in *E. coli* and purification enables a detailed biochemical analysis of the protein on the molecular level, J Steroid Biochem Mol Biol 132, 57–65. [PubMed: 22446688]
29. Xu H, and Freitas MA (2009) MassMatrix: a database search program for rapid characterization of proteins and peptides from tandem mass spectrometry data, Proteomics 9, 1548–1555. [PubMed: 19235167]
30. Xu H, Hsu P-H, Zhang L, Tsai M-D, and Freitas MA (2010) Database search algorithm for identification of intact cross-links in proteins and peptides using tandem mass spectrometry, J Proteome Res 9, 3384–3393. [PubMed: 20469931]
31. Zhang Y (2008) I-TASSER server for protein 3D structure prediction, BMC Bioinformatics 9, 40. [PubMed: 18215316]
32. de Vries SJ, van Dijk M, and Bonvin AM (2010) The HADDOCK web server for data-driven biomolecular docking, Nat Protoc 5, 883–897. [PubMed: 20431534]
33. Vickery LE (1997) Molecular recognition and electron transfer in mitochondrial steroid hydroxylase systems, Steroids 62, 124–127. [PubMed: 9029726]
34. Muller JJ, Lapko A, Bourenkov G, Ruckpaul K, and Heinemann U (2001) Adrenodoxin reductase-adrenodoxin complex structure suggests electron transfer path in steroid biosynthesis, J Biol Chem 276, 2786–2789. [PubMed: 11053423]
35. Kakuta Y, Horio T, Takahashi Y, and Fukuyama K (2001) Crystal structure of *Escherichia coli* Fdx, an adrenodoxin-type ferredoxin involved in the assembly of iron-sulfur clusters, Biochemistry 40, 11007–11012. [PubMed: 11551196]
36. de Vries SJ, van Dijk AD, Krzeminski M, van Dijk M, Thureau A, Hsu V, Wassenaar T, and Bonvin AM (2007) HADDOCK versus HADDOCK: new features and performance of HADDOCK2.0 on the CAPRI targets, Proteins 69, 726–733. [PubMed: 17803234]
37. Dominguez C, Boelens R, and Bonvin AM (2003) HADDOCK: a protein-protein docking approach based on biochemical or biophysical information, J Am Chem Soc 125, 1731–1737. [PubMed: 12580598]
38. Krone N, Grotzinger J, Holterhus P-M, Sippell WG, Schwarz H-P, and Riepe FG (2009) Congenital adrenal hyperplasia due to 11-hydroxylase deficiency--insights from two novel CYP11B1 mutations (p.M92X, p.R453Q), Horm Res 72, 281–286. [PubMed: 19844114]
39. Wu C, Zhou Q, Wan L, Ni L, Zheng C, Qian Y, and Jin J (2011) Novel homozygous p.R454C mutation in the CYP11B1 gene leads to 11β-hydroxylase deficiency in a Chinese patient, Fertil Steril 95, 1122 e1123–1126.
40. Lambeth JD, Seybert DW, and Kamin H (1979) Ionic effects on adrenal steroidogenic electron transport. The role of adrenodoxin as an electron shuttle, J Biol Chem 254, 7255–7264. [PubMed: 222762]
41. Lambeth JD, Seybert DW, Lancaster JR Jr., Salerno JC, and Kamin H (1982) Steroidogenic electron transport in adrenal cortex mitochondria, Mol Cell Biochem 45, 13–31. [PubMed: 7050653]
42. Beilke D, Weiss R, Lohr F, Pristovsek P, Hannemann F, Bernhardt R, and Ruterjans H (2002) A new electron transport mechanism in mitochondrial steroid hydroxylase systems based on structural changes upon the reduction of adrenodoxin, Biochemistry 41, 7969–7978. [PubMed: 12069587]

43. Kido T, and Kimura T (1979) The formation of binary and ternary complexes of cytochrome P-450scc with adrenodoxin and adrenodoxin reductase.adrenodoxin complex. The implication in ACTH function, J Biol Chem 254, 11806–11815. [PubMed: 227881]

44. Hara T, Koba C, Takeshima M, and Sagara Y (2000) Evidence for the cluster model of mitochondrial steroid hydroxylase system derived from dissociation constants of the complex between adrenodoxin reductase and adrenodoxin, Biochem Biophys Res Comm 276, 210–215. [PubMed: 11006108]

45. Cao PR, and Bernhardt R (1999) Modulation of aldosterone biosynthesis by adrenodoxin mutants with different electron transport efficiencies, Eur J Biochem 265, 152–159. [PubMed: 10491169]

46. Behlke J, Ristau O, Muller E-C, Hannemann F, and Bernhardt R (2007) Self-association of adrenodoxin studied by using analytical ultracentrifugation, Biophys Chem 125, 159–165. [PubMed: 16916573]

47. Urushino N, Yamamoto K, Kagawa N, Ikushiro S, Kamakura M, Yamada S, Kato S, Inouye K, and Sakaki T (2006) Interaction between mitochondrial CYP27B1 and adrenodoxin: role of arginine 458 of mouse CYP27B1, Biochemistry 45, 4405–4412. [PubMed: 16584176]

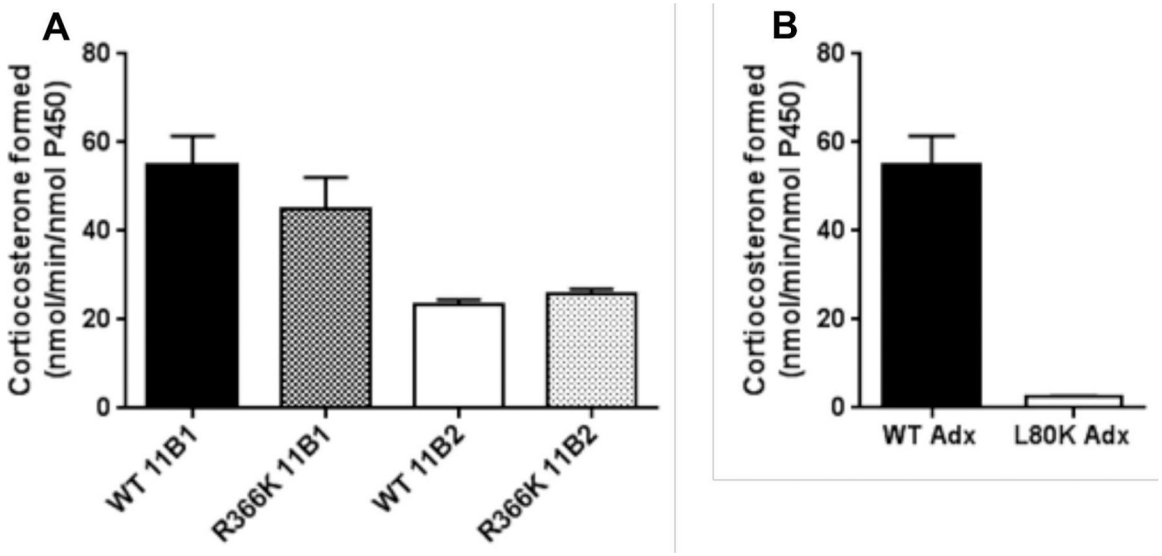

Figure 1.

(A) 11β-hydroxylase activity of P450 11B1 and P450 11B2 (WT vs. R366K) with Adx when incubated with 200 μM 11-deoxycorticosterone as described in Experimental Procedures. (B) Loss of 11β-hydroxylase activity of P450 11B1 with Adx L80K mutation. Results are shown as turnover number from triplicate determinations.

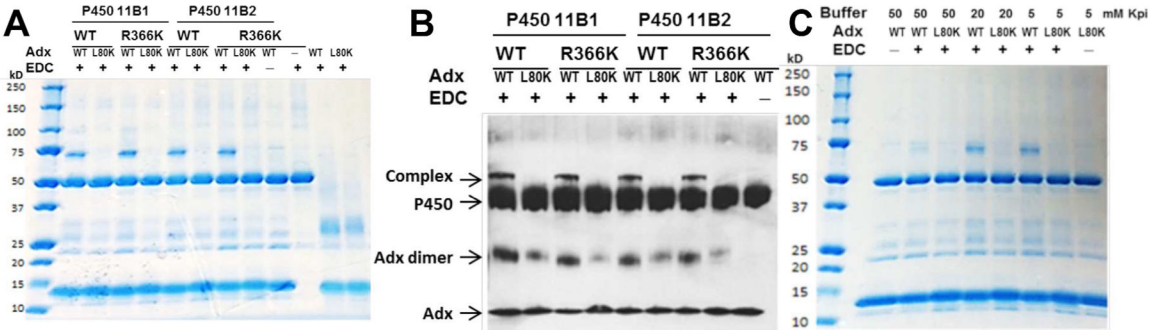

Figure 2.

SDS-PAGE, and immunoblots of P450 11B1/11B2 (WT or R366K) and Adx or mutation L80K cross-linked with EDC, and effect of ionic strength on complex formation. Aliquot of the reaction mixture was loaded in each lane and subjected to SDS-PAGE and immunoblot with anti-polyhistidine antibody, which detects both P450 11B1/11B2 and Adx. (A) P450 11B1/11B2 (50 kDa) and Adx (12 kDa), wild-type or mutations as indicated, was incubated in the absence or presence of EDC. (B) The immunoreactive bands corresponding to P450, Adx, Adx dimer, and the 1:2 P450-Adx complex ("complex") are indicated. C. Effect of ionic strength on P450 11B2 R366K-Adx_2 ternary complex formation.

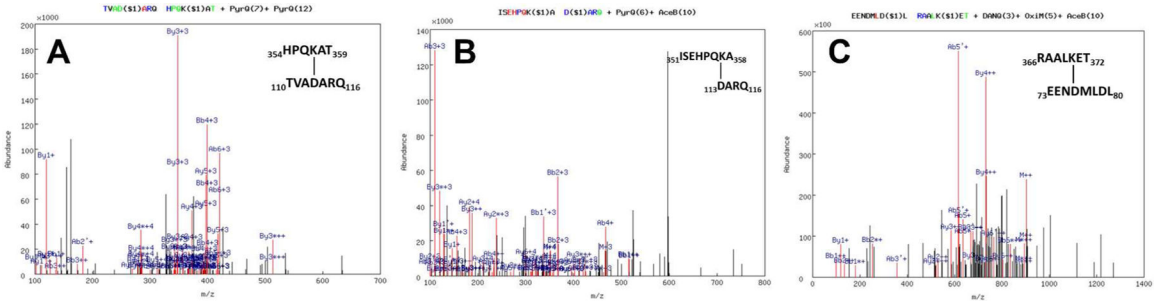

Figure 3.

Representative fragmentation spectra of cross-linked peptides between P450 11B1 and Adx identified by MassMatrix. (A) Salt bridge between K357 of P450 11B1 WT and D113 of Adx (B molecule), (B) Salt bridge between K357 of P450 11B1 R366K and D113 of Adx (B molecule), and (C) Salt bridge between K370 of P450 11B1 WT and D76 of Adx (A molecule) as determined by MS/MS spectrum of chymotryptic digests of the 74-kDa complex. The numbers designate the positions of the cross-linked peptide sequences with the cross-linked residues indicated. In the spectra, a pair of consecutive y ions is tagged in green, a pair of consecutive b ions in blue, and pairs of both consecutive y and b ions in red, whose mass difference equals the mass of the amino acid residue. Link sites are labeled by "$i" (i= 1,2…). The label at top indicates the type of modification: deamidation of NQ (DANQ), pyro-Glu from Q (PyrQ), oxidation of M (OxiM), and acetylation of N-term (AceB), and the location of the modification is indicated by the number in parentheses.

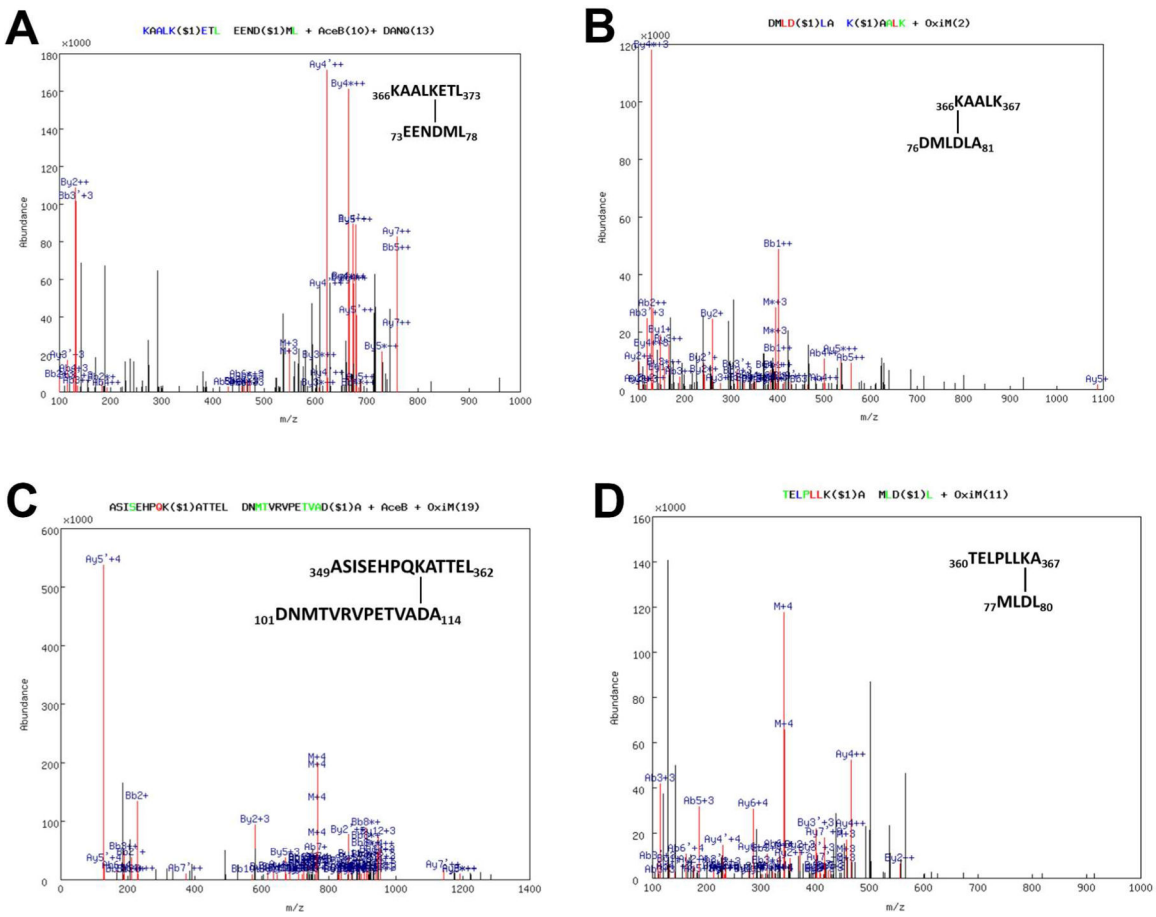

Figure 4.

Representative fragmentation spectrums of cross-linked peptides between P450 11B2 and Adx identified by MassMatrix. Cross-linked peptides between (A) K370 of P450 11B2 R366K and D76 of Adx (A molecule), (B) K366 of P450 11B2 R366K and D79 of Adx (A molecule), and (C) K357 of P450 11B2 WT and D113 of Adx (B molecule), and (D) K366 of P450 11B2 R366K and D79 of Adx (A molecule), as determined by MS/MS spectrum of chymotryptic digests of the 74-kDa complex. The numbers designate the positions of the cross-linked peptide sequences with the cross-linked residues indicated. In the spectra, a pair of consecutive y ions is tagged in green, a pair of consecutive b ions in blue, and pairs of both consecutive y and b ions in red, whose mass difference equals the mass of the amino acid residue. Link sites are labeled by “$i” (i= 1,2…). The label at top indicates the type of modification: deamidation of NQ (DANQ), oxidation of M (OxiM), and acetylation of N-term (AceB), and the location of the modification is indicated by the number in parentheses.

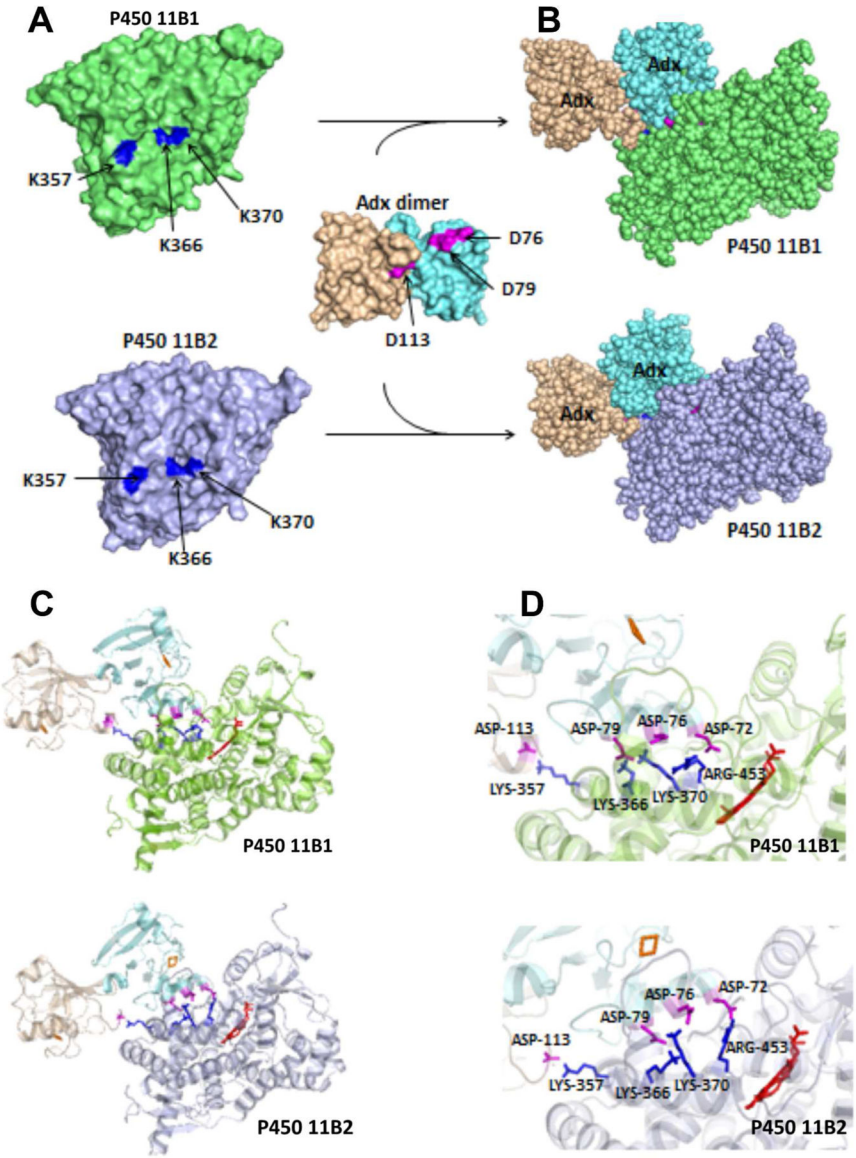

Figure 5.

Docking model of P450 11B1 and P450 11B2 with Adx dimer, based on crystal structures of P450 11B2 (PDB 4DVQ) and Adx (PDB 1CJE). The docking was performed using the programs HADDOCK, with the distance constraints of three intermolecular cross-links, K366 (P450 11B)-D79 (Adx A molecule), K370 (P450 11B)-D76 (Adx A molecule), and K357 (P450 11B)-D113 (Adx B molecule) as described in the Experimental Procedures. (A) The individual proteins are shown as a surface model, and (B) complexes formed are shown as a space-filled model. (C) Ribbon diagram of P450 11B1/11B2 interacting with Adx dimer, and (D) close-up views of the interaction interfaces. The heme in shown in red, and important residues are labeled and shown as sticks on P450 in blue and Adx in magenta.

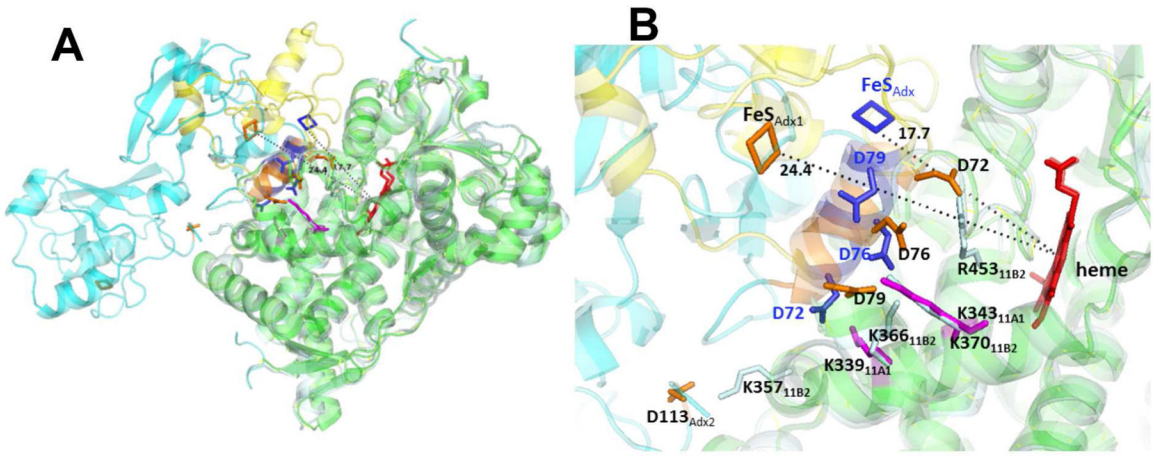

Figure 6.

Comparison of P450 11B2-R366K•Adx_2 model and P450 11A1-Adx (3N9Y) fusion protein structure. The superposition of heme moieties was performed using the PyMOL molecular graphics program. (A) Superposition of the P450 11B2-R366K•Adx_2 model (pale cyan-cyan) onto the 2.1 Å P450 11A1-Adx structure (green-yellow). (B) Close-up comparison of the P450-Adx interfaces. The heme is shown in red, and important residues are labeled and shown as sticks on P450 11B2 in pale cyan, P450 11A1 in magenta, Adx_2 dimer in orange, and fused Adx (3N9Y) in blue. Distances between metal centers are indicated.

Table 1.

Cross-linked peptide pairs between P450 11B1/11B2 and Adx (A & B molecules)

Index	Charge	PP*	PP_2	PP_{tag}	m/z	MW(obs)	MW	CYP11B1**	CYP11B2**	Adx**	Modification***
3433	4	37.3	24.1	1.7	348.1758	1389.6815	1389.6951	HPQ<u>K</u>AT		TVA<u>D</u>ARQ(B)	PyrQ
4433	3	6.7	14.0	1.8	550.2820	1648.8314	1648.8180		KAAL<u>K</u>ETL	EEN<u>D</u>ML(A)	AceB, DANQ
4924	3	16.9	14.2	3.7	402.2232	1204.6552	1204.6606		KAAL<u>K</u>	DML<u>D</u>LA(A)	OxiM
6267	4	18.3	9.6	1.4	767.8810	3068.5023	3068.4841		ASISEHPQ<u>K</u>ATTEL	DNMTVRVPETVA<u>D</u>A(B)	AceB, OxiM
6457	4	35.1	14.3	2.6	343.9506	1372.7805	1372.7756		TELPLL<u>K</u>A	ML<u>D</u>L(A)	OxiM
6990	4	28.1	14.0	4.5	351.9259	1404.6817	1404.6866	ISEHPQ<u>K</u>A		<u>D</u>ARQ(B)	PyrQ, AceB
9782	2	10.9	12.6	2.1	903.9162	1806.8251	1806.8426	RAAL<u>K</u>ET		EENDML<u>D</u>L(A)	DANQ, OxiM, AceB

*The quality of a peptide match is mainly evaluated by three statistical scores: pp, pp_2, pp_{tag}. A peptide match with max (pp,pp_2) > 3.7 and pp_{tag} > 1.3 is considered to be significant with p value < 0.05.

**The cross-linked residues are underlined.

***Variable modifications: deamidation of NQ (DANQ), pyro-Glu from Q (PyrQ), oxidation of M (OxiM), and acetylation of N-term (AceB)

Table 2.

PISA analysis of the salt-bridge and H-bonding interactions between the residues in the interface of P450 11B1 R366K and Adx

	P450 11B1 Residue (Atom)	Adx Residue (Atom)	Distance (Å)
Hydrogen Bonds			
1	ASN 437 (HD21)	LEU 50 (O)	2.01
2	ASN 152 (HD22)	GLU 65 (O)	1.83
3	GLN 449 (HE22)	ILE 70 (O)	2.30
4	ARG 453 (HHEE)	ASP 72 (OD1)	1.64
5	GLY 443 (N)	ASP 72 (OD2)	2.75
6	PHE 438 (N)	GLU 73 (OE1)	2.89
7	ARG 436 (HH11)	GLU 73 (OE1)	1.61
8	ARG 436 (HH22)	GLU 73 (OE2)	1.65
9	LYS 370 (HZ2)	ASP 76 (OD1)	1.56
10	ARG 436 (HE)	ASP 76(OD2)	1.61
11	ARG 436 (HH21)	ASP 76 (OD2)	2.40
12	LYS 366 (HZ3)	ASP 79 (OD1)	1.64
13	LYS 370 (HZ1)	ASP 79 (OE1)	1.65
14	LYS 357 (HZ2)	ALA 112 (OD2)	1.70
15	LYS 357 (HZ1)	ASP 113 (O)	1.61
16	GLU 457 (OE1)	ASN 75 (OD1)	1.97
17	GLU 361 (OE1)	ARG 115 (HD22)	1.82
18	GLU 361 (OE2)	ARG 115 (HH22)	1.64
Salt Bridges			
1	ARG 453 (NE)	ASP 72 (OD1)	3.79
2	ARG 453 (NH1)	ASP 72 (OD1)	2.64
3	ARG 436 (NH1)	GLU 73 (OE1)	2.63
4	ARG 436 (NH2)	GLU 73 (OE1)	3.50
5	ARG 446 (NH1)	GLU 73 (OE2)	3.41
6	ARG 446 (NH2)	GLU 73 (OE2)	2.65
7	LYS 370 (NZ)	ASP 76 (OD1)	2.58
8	ARG 436 (NE)	ASP 76 (OD2)	2.58
9	ARG 436 (NH2)	ASP 76 (OD2)	3.13
10	LYS 366 (NZ)	ASP 79 (OD1)	2.66
11	LYS 370 (NZ)	ASP 79 (OD2)	2.64
12	LYS 366 (NZ)	ASP 79 (OD2)	3.36
13	LYS 357 (NZ)	ASP 113 (OD1)	2.64
14	GLU 361 (OE1)	ARG 115 (NE)	2.80
15	GLU 361 (OE2)	ARG 115 (NE)	3.30
16	GLU 361 (OE1)	ARG 115 (NH2)	3.58
17	GLU 361 (OE2)	ARG 115 (NH2)	2.61

Table 3.

PISA analysis of the salt-bridge and H-bonding interactions between the residues in interface of P450 11B2 R366K and Adx

	P450 11B1 Residue (Atom)	Adx Residue (Atom)	Distance (Å)
Hydrogen Bonds			
1	ARG 453 (HH11)	ASP 72 (OD1)	1.62
2	ARG 453 (HH22)	ASP 72 (OD2)	1.75
3	LYS 370 (HZ1)	ASP 76 (OD1)	1.59
4	ARG 436 (HE)	ASP 76 (OD2)	1.68
5	LYS 370 (HZ3)	ASP 79 (OD2)	2.20
6	LYS 366 (HZ1)	ASP 79 (OD2)	1.71
7	GLN 356 (HE21)	ASP 86 (OD2)	2.03
8	LYS 357 (HZ2)	ALA 112 (O)	2.15
9	LYS 357 (HZ3)	ASP 113 (OD1)	1.67
10	GLN 155 (OE1)	ARG 87 (HH11)	1.68
Salt Bridges			
1	ARG 453 (NH1)	ASP 72 (OD1)	2.62
2	ARG 453 (NH2)	ASP 72 (OD1)	3.17
3	ARG 453 (NH1)	ASP 72 (OD2)	3.79
4	ARG 453 (NH2)	ASP 72 (OD2)	2.75
5	HIS 440 (ND1)	ASP 76 (OD1)	3.54
6	LYS 370 (NZ)	ASP 76 (OD1)	2.63
7	ARG 435 (NE)	ASP 76 (OD2)	2.67
8	ARG 435 (NH2)	ASP 76 (OD2)	3.47
9	LYS 366 (NZ)	ASP 79 (OD1)	3.84
10	LYS 370 (NZ)	ASP 79 (OD2)	3.05
11	LYS 366 (NZ)	ASP 79 (OD2)	2.73
12	HIS 354 (NE2)	ASP 86 (OD2)	3.78
13	LYS 357 (NZ)	ASP 113 (OD1)	2.68

Table 4.

Sequence alignment of mitochondrial P450s in the region of the Adx binding site*

CYP11A_HUMAN	327	D	M	A	T	M	L	Q	L	V	P	L	L	K	A	S	I	K	E	T	L	346
CYP11A_BOVIN		D	I	S	K	M	L	Q	M	V	P	L	L	K	A	S	I	K	E	T	L	
CYP11A_RAT		D	M	A	K	M	V	Q	L	V	P	L	L	K	A	S	I	K	E	T	L	
CYP11B1_HUMAN	354	H	P	Q	K	A	T	T	E	L	P	L	L	R	A	A	L	K	E	T	L	373
CYP11B2_HUMAN		H	P	Q	K	A	T	T	E	L	P	L	L	R	A	A	L	K	E	T	L	
CYP11B1_RAT		N	P	Q	K	A	M	S	D	L	P	L	L	R	A	A	L	K	E	T	L	
CYP11B2_RAT		N	P	Q	K	A	M	S	D	L	P	L	L	R	A	A	L	K	E	T	L	
CYP11B1_BOVIN		N	P	Q	R	A	I	T	E	L	P	L	L	R	A	A	L	K	E	T	L	
CYP27A_HUMAN		P	Q	H	K	D	F	A	H	M	P	L	L	K	A	V	L	K	E	T	L	
CYP27B_HUMAN	358	P	S	A	T	V	L	S	Q	L	P	L	L	K	A	V	V	K	E	V	L	377

*The lysine residues involved in electrostatic interactions are highlighted with cyan and arginine with gray

Table 5.

Interaction sites identified by crystal structure, chemical cross-linking, and site-directed mutagenesis of Adx, ferredoxin reductase and P450s

Adx Residue*	Interaction site on P450 isozyme and reductase					References
	11A1	11B1	11B2	27B1	FdR	
D39					K27	[34]
D72	K339	R453	R453	K370/K374	R244	[23, 34, 47, this paper]
E73	K339	R436				[23, this paper]
E74				K370/K374		[47]
D76	K343	K370	K370/R436	R458	R240	[23, 34, 47, this paper]
D79	K406	R366/K370	R366/K370	R457	R211	[23, 34, 47, this paper]
D113**		R357	R357			[this paper]
E116					R370	[34]

*Positions are numbered according to the crystal structure of human Adx (PDB 3P1M)

**Second Adx molecule